THE RUSSULA ROLLING STAND: A NEW DESIGN AND FEM ANALYSIS[1]

Marco Fulgosi[2]
Marco Zeni[3]

Abstract
Today´s "housing-less Stand", in long product rolling technology, is the preferred type of rolling mill stand used by most steel producers worldwide. The rolling unit includes a stand nucleus with four chocks that are kept together by four threaded stay bolts. The rolling unit is supported by a stand holder and the whole assembly can be shifted sideways in order to keep the rolling line fixed. The housing-less stands due to their compactness, technological features and choice of materials, are considered the most suitable to obtain superior finished product tolerances. This paper analyzes the interaction between the threaded stay bolt and the chock during rolling. Traditionally such interaction takes place in a spherical joint; however, practical experience shows that the interaction occurs systematically perpendicular to the rolling axis. Russula has studied the issue and created a joint that optimizes the roller bearing behavior under load, which increases the roller bearing life. The relative contact between the parts occurs on a cylindrical joint, perpendicular to the rolling axis. An FEM analysis has been performed on two stand sizes (neck diam. 200mm and 280mm). A comparison between the spherical and the cylindrical setups shows that both solutions are valid whereas the cylindrical setup works with a lower contact specific pressure on the joint, which is beneficial to the uniform distribution of the rolling load inside the main bearings.
Key words: Rolling stand; Housingless stand; FEM analysis; Models.

[1] *Technical contribution to the 50th Rolling Seminar – Processes, Rolled and Coated Products, November, 18th to 21st, 2013, Ouro Preto, MG, Brazil.*
[2] *Senior Mechanical Engineer, Russula Italia, Udine, Italy*
[3] *General Manager, Russula Italia, Udine Italy*

1 INTRODUCTION

Based on 25 years' experience in rolling processes and technology, Russula launches its own housing-less stand. Two aspects of the stand design were focused on. First is the quality of the components which are manufactured in selected workshops in Europe. The second aspect is the generous dimensioning criteria. The rolling stand is equipped with the latest technological features such as:

- Symmetrical gap adjustment of each rolling unit by remote control from the main pulpit to minimize the number of manual operator interventions along the mill line.
- Four rows of roller bearings for an even distribution of the rolling load on the roll necks and axial thrust bearings to keep control of the axial forces generated by asymmetric rolling forces.
- Self-balancing weight system for the spindles supporting group.
- Quick locking and unlocking system for the rolling unit
- Precise axial regulation system for the top roll
- On board wheel type carriage to allow stand interchangeability between horizontal and vertical arrangements
- Back-lash elimination with maintenance free mechanical spring balancing system.

The 3D rendering in Figure 1 below is showing the above mentioned construction details.

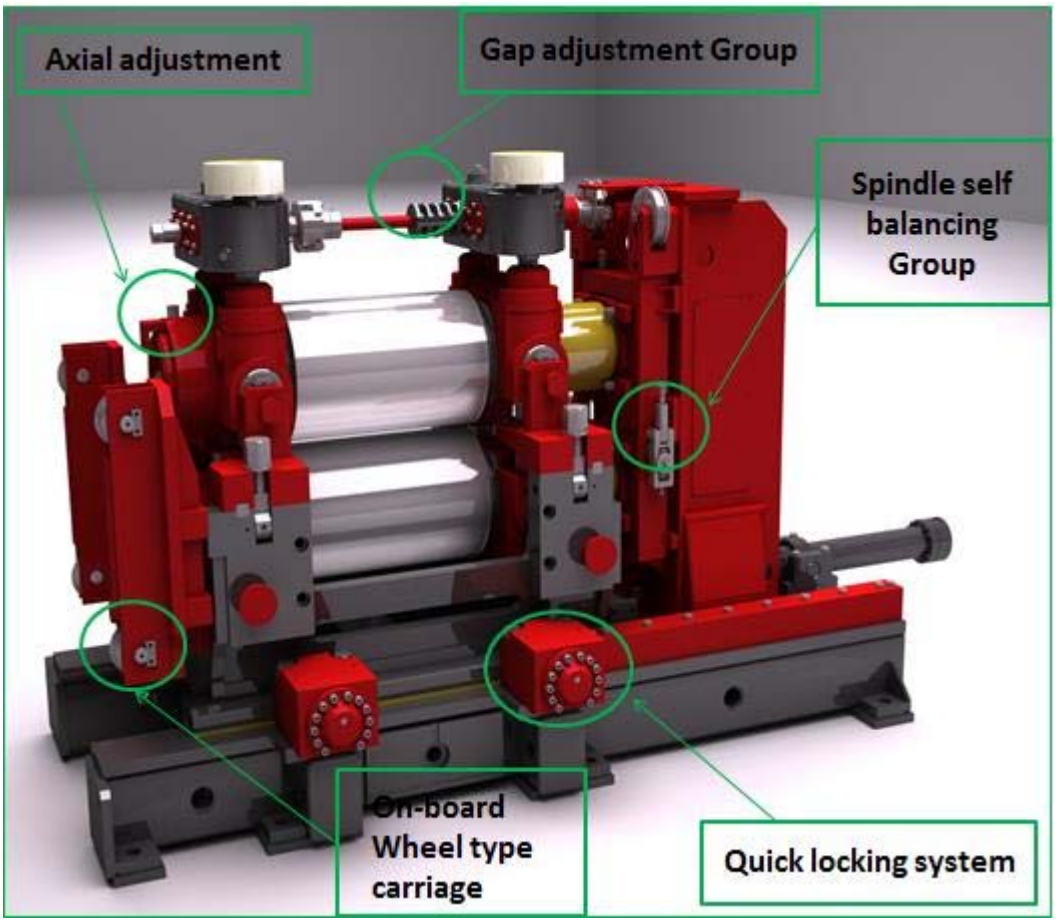

Figure 1: 3D rendering of the Russula stand.

2 MATERIAL AND METHODS

The compactness of the design along with a reduced equipment weight optimizes the auxiliary rolling mill equipment supply. This design reduces the rolling mill foundation thickness, the crane load capacity and the space requirements for ordinary maintenance operations.

2.1 Component Quality

Selected materials for the rolling stand components were used to obtain the best results from an operational and endurance point of view. For the key components we adopt the following criteria:

- Chocks and nucleus supporting foot are made out of casted steel type FeG52Vr annealed steel with HB 160-175, to guarantee the stability of the material.
- Stay bolts for the gap adjustment are made out of AISI 420 stainless steel and are hardened and tempered in order to guarantee perfect sliding and to avoid material oxidation.
- The bronze hubs for the gap adjustment group are made out of alloyed steel heat treated type 42CrMo4, with a surface treatment, case-hardened and grinded.
- On board mechanical parts are made out of steel type C46 and are hardened, tempered and Chrome plated where necessary.
- The axial regulation components are Nickel-teflon treated to facilitate reciprocal sliding.
- The threaded bronze bushing used for the regulation of the roll gap is made out of Centrifuged steel type G-CuAl11Fe4Ni4 with HB 190 – 220.
- The rolls adjustment group on the top of the stand is made out of mechanical cast iron type EN-GJS-500-7 in order to guarantee the mechanical property and the stability of the material in the long run.
- The worm screw mechanism of the rolls adjustment group is made out of case-hardened and tempered steel type 36CrNiMo4 with HB 250-280 coupled to bronze gear type CuAl10Fe5Ni5-C-GC suitable to bear exceptionally high loads.

2.2 Generous Dimensioning

The second key factor that we have considered in the designing of the rolling mill stand is the generous dimensioning of each single stand component in order to guarantee the longest life of all the components subject to wear and tear as well as to facilitate maintenance at prolonged time intervals. This aspect is consistent with the behavior of the rolling stand for an extended life of the critical components as it will be demonstrated by the enclosed analysis, which has been developed in cooperation with the University of Udine.
The investigation has been carried out for one of the most critical aspects related to the deformation generated by the rolling force on the rolling unit mechanical components, which are transferring the rolling load to the mechanical elements responsible for bearing such load.

2.3 Analysis Objective

This paper analyzes the interaction between the threaded stay bolts and the chocks during rolling. Traditionally such interaction takes place in a spherical joint; however, practical experience shows that the interaction occurs systematically perpendicular to the rolling axis. The company studied the issue and created a joint that optimizes the roller bearing behavior under load, thus increasing the roller bearing life as it will be demonstrated in the following considerations. The relative contact between the parts occurs on a cylindrical joint, perpendicular to the rolling axis.
An FEM analysis has been performed on two stand sizes (neck diam. 200mm and 280mm). A comparison between the spherical and the cylindrical setups shows that both solutions are valid whereas the cylindrical setup works with a lower contact specific pressure on the joint, which is beneficial to the uniform distribution of the rolling load inside the main bearings.
By evaluating a three-dimensional mathematical model based on the finite element method, the mechanical behaviour of a rolling stand can be modelled. Particular attention was given to the computation of the overall stiff ness and to the contact pressure distribution in the coupling elements of the chock. Two different design configurations, named respectively S and C were considered, which refer to the coupling solution based on a spherical slider or on a cylindrical slider respectively. Two rolling stand sizes were also considered, indicated as 200 and 280 respectively, which corresponds to the roll neck diameter. In conclusion the following 4 models were considered:

- 200S: rolling stand with 200 mm roll neck size, spherical slider
- 200C: rolling stand with 200 mm roll neck size, cylindrical slider
- 280S: rolling stand with 280 mm roll neck size, spherical slider
- 280C: rolling stand with 280 mm roll neck size, spherical slider.

2.3 Description of the Models

The geometry of the rolling stand is quite complex (see Figure 2), for the purpose of the analysis stand will be broken down into by 3 types of elements:

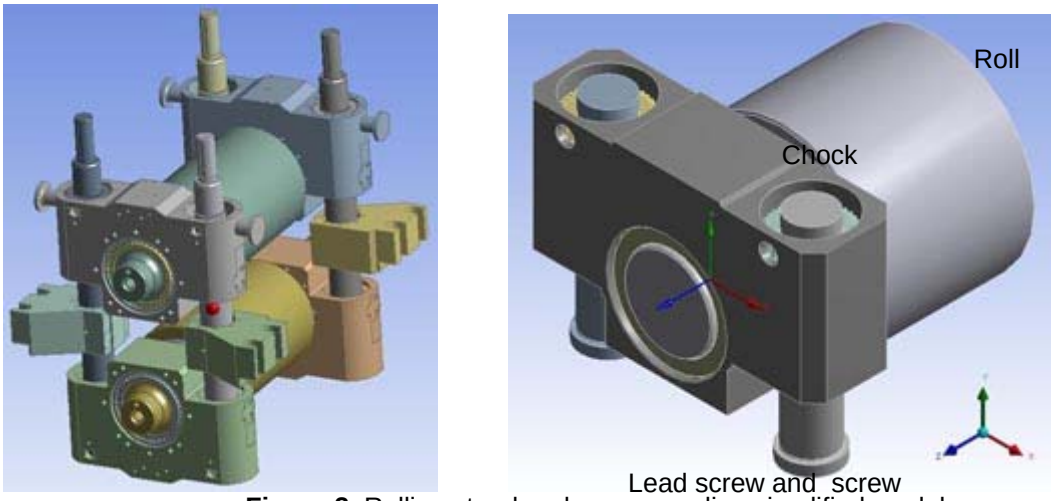

Figure 2: Rolling stand and corresponding simplified model.

1) The chock is a steel structure characterized by a complex geometry. Its function is to support the two working rolls, thus permitting the rolling forces to be counterbalanced. The external ring of the working roll bearing is supported inside a hole. The slide is supported inside 2 cylindrical holes, which can have a spherical or cylindrical geometry. The sliders couple with the corresponding surfaces (spherical or cylindrical) on the screw element.
2) Screw and lead screw: it can be considered constituted by a screw, a lead screw coupled to an element with respectively a spherical or cylindrical surface witch couples with the corresponding slider in the chock.
3) Working roll: it is constituted by a cylindrical shaped element; the bearing is represented by a hollow cylinder.

Four chocks, four screw elements and two working rolls constitute each rolling stand; as the structure is characterized by two planes of symmetry, only one quarter of the structure was considered. In summary the model is constituted by one chock, two screw elements and half a roll (see Figure 2 3D rendering on the right).
The materials of the components and their respective properties are listed below for each type of element; the material was assumed to have a linear elastic behaviour.

2.3.1 Materials of the components

- Chock + spherical slider form one piece: steel
- Screw : steel
- Lead screw: bronze
- Cylindrical slide: steel
- Bearing: steel
- Roll: cast iron

2.3.2 Material properties

- Steel: E = 200 GPa, $\nu = 0.3$
- Bronze: E = 100 GPa, $\nu = 0.32$
- Cast iron: E = 180 GPa, $\nu = 0.26$

Constraints: besides the symmetry conditions, contact between the cylindrical and the spherical surfaces were imposed, with a null coefficient of friction.
Loads: the rolling force was applied in the middle point; this force amounted to 1600 kN for the 200 size rolling stand and 4000 kN for the 280 size rolling stand. In consideration of the symmetry problem, a halved load was applied (800 and 2000 kN).
Mesh: the FEM model was mainly constituted by 10-node tetrahedral elements and some 20-node hexahedral elements. An overall view of the final mesh is shown in Figure 3, for two cases, 200S and 200C. Figures 4 and 5 show in detail the meshes of the main components.

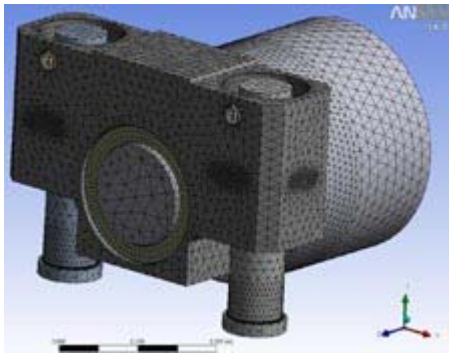

a) 200S

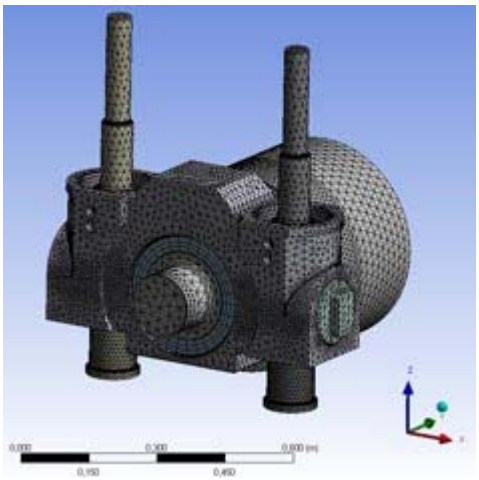

b) 200C

Figure 3: Overall view of the FEM model (200S & 200C).

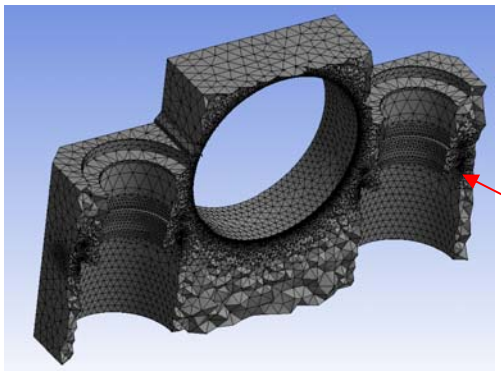

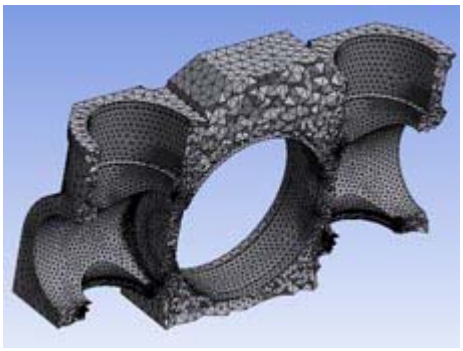

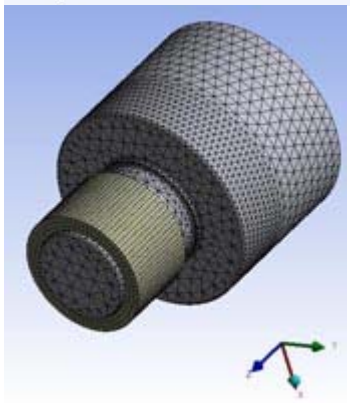

c) 200S

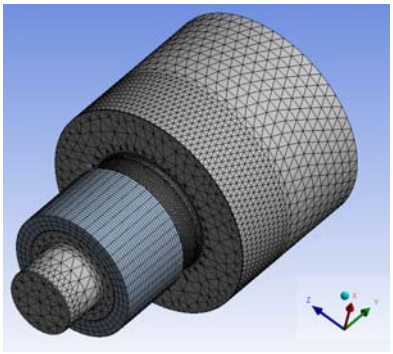

d) 200C

Figure 4: Close up view of the chock and roll element models (200S & 200C).

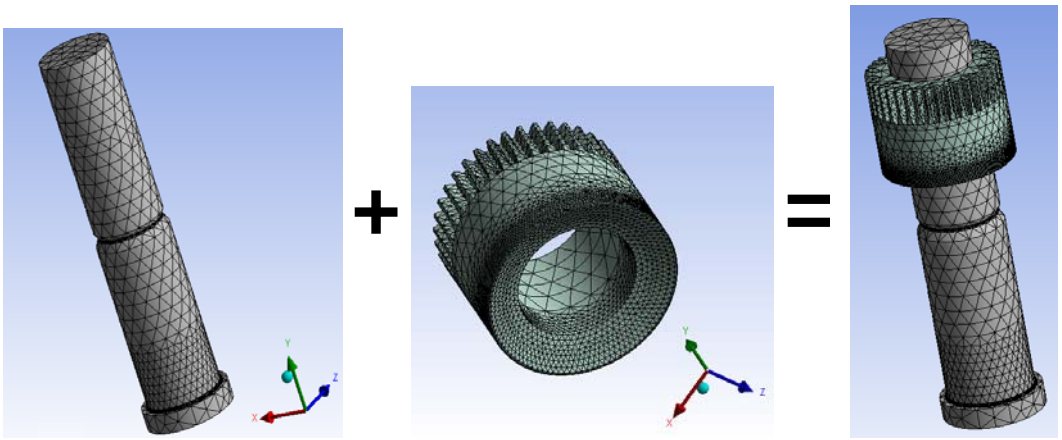

a) 200S

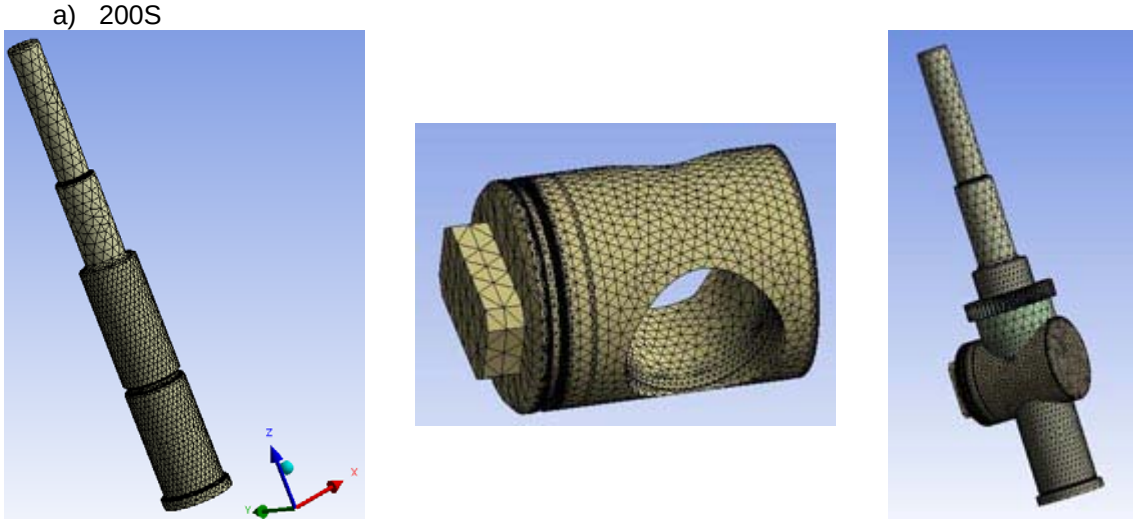

b) 200C

Figure 5: Close up view of the screw and lead screw element model (200S & 200C).

3 RESULTS AND DISCUSSION

3.1 Results of the FEMAnalysis

In consideration of the non linearity of the problem due to the contact and the large model dimension, an optimized mesh was obtained iteratively. First a linear analysis was performed with refinement in order to guarantee convergence of the main engineering parameters. Subsequently a non-linear analysis was performed while the mesh was refined only in the contact zone, up to convergence. The convergence analysis was performed in terms of Von Mises stress in the case of stress concentrators (roll fillet) and in term of contact stresses in the contact nonlinear analysis; convergence was achieved when relative error between two consecutive mesh refinements were less than 5%. The following parameters were considered: rolling stands overall stiffness, stress concentration on the roll and contact pressure on the sliders.

3.2 Rolling Stand Stiffness

Figures 6 and 7 demonstrate an exaggerated deformed shape of the structure (scale factor 150x) for the 4 cases. It was observed that the overall deformation of the structure is due mainly to the roll bending and to the deformation of the chock.

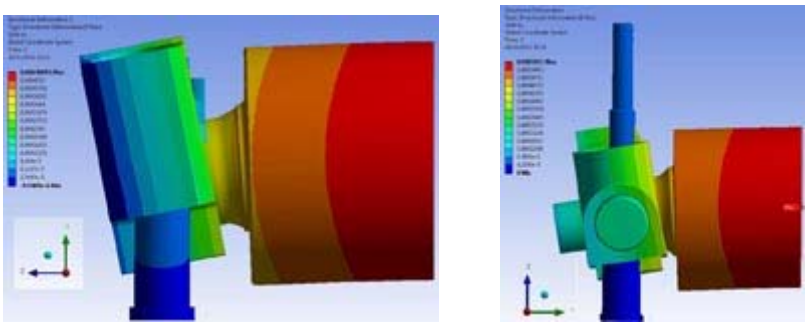

Figure 6: Overall deformed shape of the rolling stand, 200S and 200C configuration.

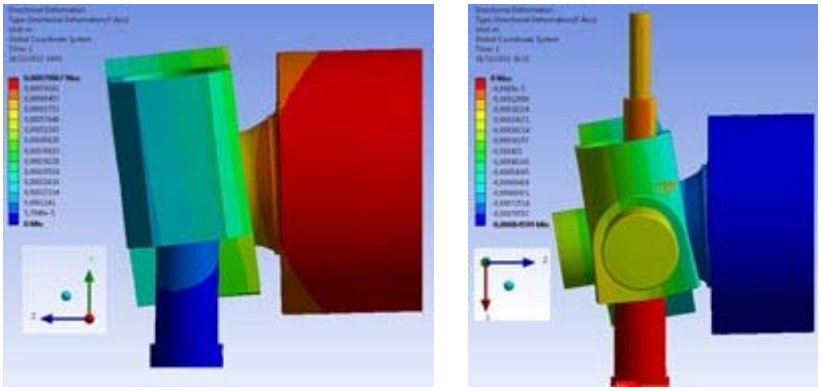

Figure 7: Overall deformed shape of the rolling stand 280S and 280C configuration.

The overall stiffness *K* of the structure was obtained simply considering the ratio between the applied load *F* and the corresponding vertical displacement *f* of the roll middle surface at the upper edge; in the case of the 200S a vertical displacement of 0.49 mm was obtained, corresponding to a stiffness $K=F/f$= 1600000/0.49= 326 MN/mm.

If the same approach is applied for the 4 cases the following results were obtained:

200 S: K= 3,26 MN/mm

200 C K= 2,90 MN/mm

280 S K= 5.00 MN/mm

280 C K= 4.76 MN/mm

Due to the larger roll diameter, the 280 case shows a higher stiffness with respect to the 200 case. By comparing the spherical and the cylindrical configurations, it was concluded that in both cases the spherical coupling permits a slightly higher stiffness to be achieved.

In order to evaluate the influence of the bearing stiffness, that is not provided by the equipment supplier, a sensitivity analysis was performed for the 200S case; the bearing is modelled as a hollow cylinder of metal with different modulus of elasticity (one half and one quarter of that of steel): two different ratio *r* between the stiffness of the bearing k_{si} and an unknown bearing stiffness k_0 was considered.

Under F=1600 kN the following values of overall stiffness k_f were obtained.

For $r= k_{s1}/ k_0$ =0.5, f=0.60124 mm, k_f =2.662 MN/mm

For $r= k_{s2}/ k_0$=0.25, f =0.61745 mm, k_f =2.590 MN/mm

As the resultant stiffness of the rolling stand and bearing is:

$$\frac{F}{v} = k_t = \frac{1}{\frac{1}{k_b}+\frac{1}{k_g}} \text{ which means: } k_t = \frac{1}{\frac{1}{rk_0}+\frac{1}{k_g}}$$

where k_b is the bearing stiffness and k_g is the rolling stand stiffness without the bearing, it follows that, for the two considered cases, k_0 and k_g can be evaluated, resulting in values of k_0 two order of magnitude higher than that of the overall stiffness, thus proving that the choice of this parameter does not influence the behaviour of the system. In fact:

$$k_0 = \frac{2}{\frac{1}{k_{t2}} - \frac{1}{k_{t1}}} = 1.9741e8 \text{ N/mm} \approx 2e8 \text{ N/mm} >> k_t$$

3.3 Stress Concentration on the Roll

Stress concentration on the roll showed that the contact distribution in the slider does not influence significantly the stress distribution on the roll; as a consequence it was possible to perform a linear analysis at increasing levels of mesh refinement in the fillet region up to convergence. The results are reported in Figure 8.

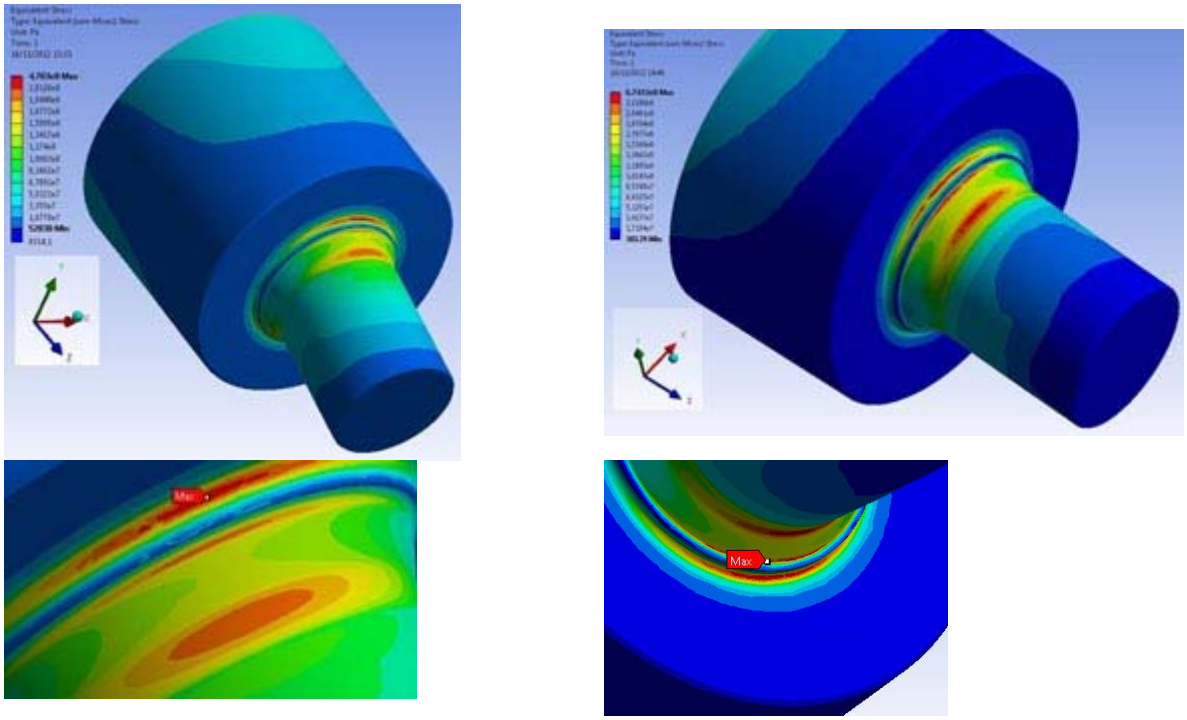

Figure 8: Stress distribution in the fillet of the working roll 200S and 280S.

In particular, in the case of the roll with diameter 200 a maximum von Mises stress of 470 MPa arised in proximity to the fillet closest to milling roll, while the 280 maximum von Mises stress is located on the intermediate fillet and has a value of 670 MPa. These results are not affected by the adopted slider solution.

3.4 Contact Pressure Distribution in the Slider

The contact pressure in the slider was thoroughly studied, in particular with the aim of comparing the two solutions: spherical and cylindrical couplings.
In the case of the spherical coupling (200S and 280S) a similar behaviour was observed. As shown in Figure 9 the pressure distribution on the slider were quite uniform, only with a slight peak in the inner part, closer to the vertical symmetry plane, of the outer edge, probably due to a geometrical effect.

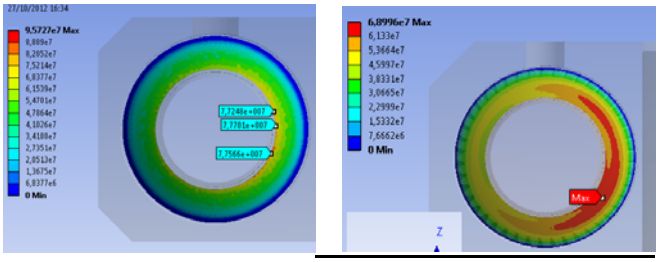

Figure 9: Pressure distribution on the spherical slider (200S left, 280S right).

In the case of the cylindrical coupling as shown in Figure 10, the pressure distribution is significantly less uniform. In particular in the inner side (closer to the chock vertical plane of symmetry) there is a high pressure concentration peak.

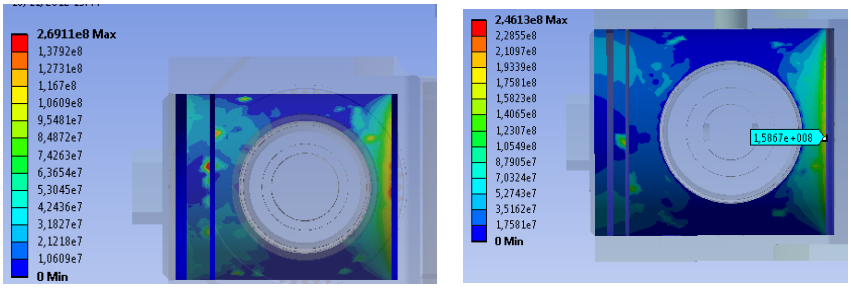

Figure 10: Pressure distribution on the cylindrical slider (200C left, 280C right).

Figure 11 shows the parts of the slider surface that are in contact (brown colour) and the parts of the slider surface where contact does not occur (yellow colour). The test demonstrates that the contact is not uniform on the whole surface, when the load is applied. Further tests were performed at different fractions of the final load (see Figure 12) to clarify that this is a regressive type contact which shows, when a initial load is applied, a sudden reduction of the contact surface that stabilizes when the load increases.

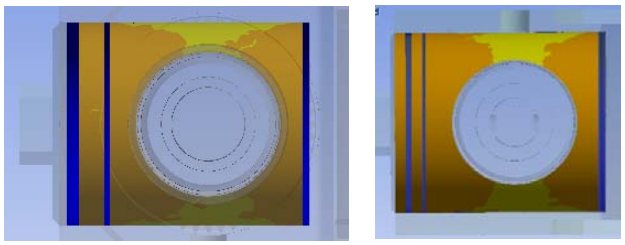

Figure 11: Contact surface on the cylindrical slider (200C left, 280C right).

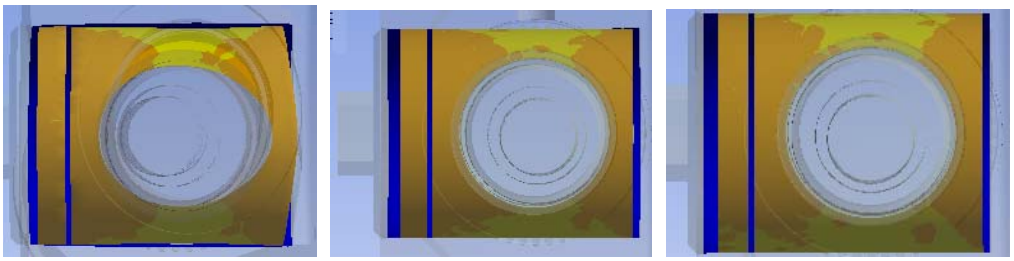

Figure 12: Contact surface (200C) respectively for 100%, 50% and 25 % of the final load.

The different behaviour of the cylindrical coupling with respect to the spherical coupling was easily understood if the overall rolling mill deformation is considered.

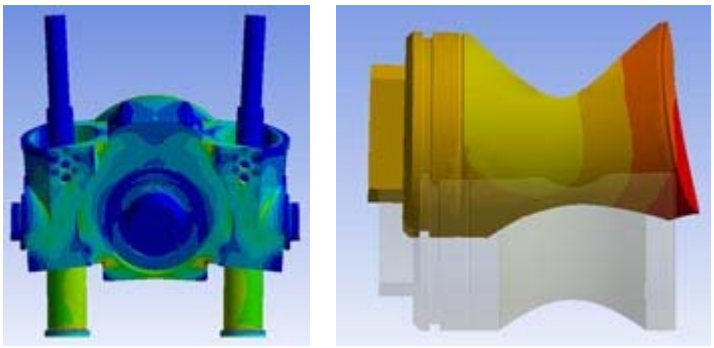

Figure 13: Deformation of the overall structure and of the cylindrical slider (200C).

The chock bends (Figure 13 left), and as the cylindrical slider does not permit rotation, a bending moment is transferred to the screws; this bending moment produces a pressure distribution that increases in the inner side. In particular, the cylinder bends (Figure 13 right) mainly in the central less stiff portion, therefore the contact does not occur in the central part. In addition localized contact points also appear on the upper surface. In Table 1 the values of contact pressure are reported in the four cases. in the S case the ratio between maximum pressure p_{max} and average pressure p_{avr} is significantly lower with respect to that obtained in the cylindrical solution; on the other hand the cylindrical solutions always has lower values of p_{avr}, thus reducing the gap among the two design solutions.

Table 1.

	p_{max} [MPa]	p_{avr}[MPa]	p_{max}/ p_{avr}
200S	77	35	2.0
280S	69	43	1.6
200C	126	26	4.8
280C	165	30	5.5

Lastly a final test was performed to determine if an increase in the chock stiffness could reduce the pressure peak in the C version. Table 2 shows the results obtained if the modulus of elasticity of the chock material E is increased. Despite a 50% E increase the maximum pressure decrease is negligible in the 200 case and decreases 20% in the 280 case.

Table 2.

Size	E [GPa]	p_{max} [MPa]	p_{avr}[MPa]	p_{max}/ p_{avr}
200	200	126	26	4.8
	300	123	26	4.7
280	200	165	30	5.5
	300	128	30	4.3

4 CONCLUSIONS

The rolling stand mechanical behaviour was studied using a non-linear analysis with the finite element method; two sizes (200 and 280) and two different design solutions (spherical and cylindrical coupling) were considered. Results showed that the 200 rolling stand has a lower stiffness with respect to the 280 one; the two coupling solutions do not affect significantly the overall stiffness.

As usual, significant stress concentrations occur in proximity to the roll fillet, the obtained values are not affected by the model non linearity and therefore can be scaled with the load. The contact pressure in the coupling at the chock and the screw is significantly different for the two cases; in the spherical slider the pressure distribution is quite uniform and the peak value is double the average value. In the case of the cylindrical slider, peaks of more than five times the average pressure occur. These pressure peaks are quite localized and this coupling is characterized by a lower value of average pressure with respect to the spherical one.
This last consideration demonstrates that a lower average pressure on the coupling can be referred to as a standard working condition for the rolling unit. In such case the lower average pressure permits a better distribution of the load on the roller bearing and therefore the roller bearing life benefits from this practical occurrence.

Acknowledgements

Department of electrical, Management and Mechanical Engineering of Udine.

BIBLIOGRAPHY

1 K.J. Bathe and E.L. Wilson, *Numerical methods in finite element analysis*, Prentice Hall, 1976.
2 K.J. Bathe, *Finite element procedures in engineering analysis*, Prentice Hall, Inc., Englewood Cliffs, 1982.
3 O.C. Zienkiewicz, R. L. Taylor, *The Finite Element Method for Solid and Structural Mechanics*, Butterworth-Heinemann, 2005.